A TRIDENT SCHOLAR PROJECT REPORT

NO. 442

Computational Sensitivity Analysis for the Aerodynamic Design of Supersonic and Hypersonic Air Vehicles

by

Midshipman 1/C David A. Stevens, USN

UNITED STATES NAVAL ACADEMY
ANNAPOLIS, MARYLAND

USNA-1531-2

U.S.N.A. --- Trident Scholar project report; no. 442 (2015)

Computational Sensitivity Analysis for the Aerodynamic Design of Supersonic and Hypersonic Air Vehicles

by

MIDN 1/C David A. Stevens
United States Naval Academy
Annapolis, Maryland

_____

(signature)

Certification of Advisers Approval

Associate Professor Chris L. Pettit
Aerospace Engineering Department

_____
(signature)

_____
(date)

Acceptance for the Trident Scholar Committee

Professor Maria J. Schroeder
Associate Director of Midshipman Research

_____
(signature)

_____
(date)

USNA-1531-2

REPORT DOCUMENTATION PAGE

Form Approved
OMB No. 0704-0188

1. REPORT DATE *(DD-MM-YYYY)*	**2. REPORT TYPE**	**3. DATES COVERED** *(From - To)*
05-18-2015		

4. TITLE AND SUBTITLE
Computational Sensitivity Analysis for the Aerodynamic Design of Supersonic and Hypersonic Air Vehicles

5a. CONTRACT NUMBER

5b. GRANT NUMBER

5c. PROGRAM ELEMENT NUMBER

6. AUTHOR(S)
Stevens, David Arthur

5d. PROJECT NUMBER

5e. TASK NUMBER

5f. WORK UNIT NUMBER

7. PERFORMING ORGANIZATION NAME(S) AND ADDRESS(ES)

8. PERFORMING ORGANIZATION REPORT NUMBER

9. SPONSORING / MONITORING AGENCY NAME(S) AND ADDRESS(ES)
U.S. Naval Academy
Annapolis, MD 21402

10. SPONSOR/MONITOR'S ACRONYM(S)

11. SPONSOR/MONITOR'S REPORT NUMBER(S)
Trident Scholar Report no. 442 (2015)

12. DISTRIBUTION / AVAILABILITY STATEMENT

This document has been approved for public release; its distribution is UNLIMITED.

13. SUPPLEMENTARY NOTES

14. ABSTRACT

The conceptual design of hypersonic air vehicles relies on computational methods to produce estimates of aerodynamic, structural, thermal protection, and propulsion design requirements. Solving the design optimization problem presented by these competing requirements using traditional low-fidelity vehicle models and flow simulations is inadequate because these models represent the underlying physics of the combined disciplines poorly. In order to assess the potential of using physically-accurate flow simulation tools and high-resolution geometry modeling tools in the conceptual design stage, the sensitivity of a hypersonic air vehicle's lift-to-drag ratio to geometric variations was calculated using a computational framework developed for this project. The framework is unique in its integration of modern design tools such as parametric vehicle geometry models, Eulerian flow simulations with automated volumetric mesh generation and refinement, Kriging response surface generation, and global sensitivity analysis. The sensitivity of a hypersonic vehicle's lift-to-drag ratio to changes in two planform parameters was completed and demonstrated the capabilities of the framework to perform global sensitivity analyses. When the design space was extended to nine geometric parameters, the initial application of the framework failed and the results of the global sensitivity analysis were inconclusive.

15. SUBJECT TERMS
hypersonic, sensitivity analysis, Cart3D, OpenVSP, Kriging

16. SECURITY CLASSIFICATION OF:			**17. LIMITATION OF ABSTRACT**	**18. NUMBER OF PAGES**	**19a. NAME OF RESPONSIBLE PERSON**
a. REPORT	**b. ABSTRACT**	**c. THIS PAGE**		49	**19b. TELEPHONE NUMBER** *(include area code)*

The conceptual design of hypersonic air vehicles relies on computational methods to produce estimates of aerodynamic, structural, thermal protection, and propulsion design requirements. Solving the design optimization problem presented by these competing requirements using traditional low-fidelity vehicle models and flow simulations is inadequate because these models and flow simulations represent the underlying physics of the combined disciplines too poorly to be dependable. In order to assess the potential of using physically-accurate flow simulation tools and high-resolution geometry modeling tools in the conceptual design stage, the sensitivity of a hypersonic air vehicle's lift-to-drag ratio to geometric variations was calculated using a computational framework developed for this project. The framework is unique in its integration of modern design tools such as parametric vehicle geometry models, Eulerian flow simulations with automated volumetric mesh generation and refinement, Kriging response surface generation, and global sensitivity analysis. The sensitivity of a hypersonic vehicle's lift-to-drag ratio to changes in two planform parameters was completed and demonstrated the capabilities of the framework to perform global sensitivity analyses. When the design space was extended to nine geometric parameters, the initial application of the framework failed and the results of the global sensitivity analysis were inconclusive. The global sensitivity analysis failed due to the sparse sampling of the design space, the large range of each design parameter, the large interaction effects between design variables caused by the non-linearities of hypersonic flow, and the interpolation imposed by the Kriging response surface in a case with greater design parameter interactions than were expected.

Keywords: hypersonic, sensitivity analysis, Cart3D, OpenVSP, Kriging

Acknowledgments

I would like to acknowledge the guidance of Dr. Chris Pettit who fostered my initial research interests and helped at all stages of research. I am also grateful for the help and support I received from the staff of the Aerospace Systems Directorate at the Air Force Research Lab, including Dr. Phil Beran, Dr. Chris Schrock, Mr. Jim Tancred, and Mr. Dan Galibrath. They provided the technical expertise I needed to overcome the inevitable research setbacks and to guide my research towards meaningful results.

Contents

Nomenclature

AFRL	Air Force Research Laboratory
a_∞	Freestream speed of sound, $a_\infty = \sqrt{\gamma R T_\infty}$
b	Wing span
c	Chord length
c_r	Root chord length
CAD	Computer aided design
Cart3D	CFD software
CFD	Computational fluid dynamics
C_L	Coefficient of lift, $C_L = \frac{L}{q_\infty S}$
$C_{L,\alpha}$	Lift-curve slope, $\frac{\partial C_L}{\partial \alpha}$
D	Drag force
GHV	Generic Hypersonic Vehicle
GUI	Graphical User Interface
HiFire	Hypersonic International Flight Research Experimentation Program
L	Lift force
L/D	Lift-to-drag ratio
LHS	Latin hypercube sampling
MATLAB	Matrix Laboratory, a numerical programming language
M_∞	Freestream Mach number, $M_\infty = \frac{V_\infty}{a_\infty}$
OpenVSP	Open Vehicle Sketch Pad
q_∞	Freestream dynamic pressure, $q_\infty = \frac{1}{2}\rho_\infty V_\infty^2$
R	Specific gas constant
S	Planform reference area
S_i	First-order sensitivity index for the i^{th} model parameter
S_{Ti}	Total sensitivity index for the i^{th} model parameter
T_∞	Freestream temperature
V_∞	Freestream velocity
α	Angle of attack
Γ	Dihedral Angle
γ	Ratio of specific heats
ϑ	Kriging response surface smoothing parameter
θ	Wing mounting angle
ρ_∞	Freestream density
φ	Fin rotation angle

Subscript

0	Baseline parametric value
f	Fin parameter

1) Introduction

a) Background and Motivation

Research into hypersonic air vehicles is being undertaken in the United States, Europe, and elsewhere owing to the promise of allowing routine and inexpensive access to space [1].[1] Additionally, the U.S. military is also looking towards hypersonic air vehicles as a means to strike time-dependent targets before they are hidden away [2]. However, various technical challenges in vehicle systems such as control, structure, and propulsion continue to impede the development of practical hypersonic air vehicles that can perform routine operations. The individual challenges of each of these systems are compounded by interactions between these systems, e.g. the interaction of the structural system and the propulsion system in the vehicle's engine mounting. These interactions have two effects on the design of the air vehicle. First, the interactions of air vehicle systems lead to conflicting constraints for a proposed vehicle design. For example, while one design may meet a specified aerodynamic performance objective that same design may fail to meet a second structural objective. Second, the interaction of these systems can lead to unanticipated phenomena later in the development cycle that result in cost overruns or catastrophic failures in full-scale tests.

Overcoming both of these challenges requires the use of design methods that provide the designer with detailed information to aid in the ranking of design factors by their impact on the vehicle's performance [4]. High-resolution flow simulation schemes in the form of modern CFD (computational fluid dynamics) tools provide the designer with more detailed and accurate foresight of performance throughout the flight envelope. Global SA (sensitivity analysis)

[1] Hypersonic refers to flight above five times the speed of sound. For reference, the SR-71 Blackbird, the fastest manned airbreathing typically flew at three times the speed of sound.

methods provide the designer with a means to rank design factors based on upon their influence on the vehicle design. This factor ranking provides partial solutions to both of the aforementioned problems by providing the designer with deeper insight into the vehicle's characteristics. Both methods provide specific advantages to solving the problems of conflicting design constraints and predicting otherwise unanticipated phenomena.

In the case of conflicting design constraints, factor ranking provides the designer a means to identify which factors should be optimized in order to achieve the performance objectives. Factor ranking addresses unanticipated phenomena by providing the designer a means to identify which factors play a large role in the vehicle's performance and may need to be constrained in later designs to avoid undesirable operating characteristics. However, factor ranking from sensitivity analysis based on a low-fidelity model might be misleading, especially when the design cruise condition is hypersonic. Strong shock waves, real gas effects, and high thermal loads that are missed by the simulations will result in poorly optimized and possibly dangerous designs.

High-resolution flow simulations must be carried out along with factor ranking to provide a solution to the problems of vehicle optimization with conflicting design constraints and avoiding unanticipated phenomenon. In the case of conflicting design constraints, high-resolution flow simulations provide the capability to assess designs not so severely hampered by the limitations or assumptions inherent to low-fidelity flow simulations. This affords designers more flexibility to explore novel vehicle designs early on, and thereby improve the chance of uncovering configurations that offer better performance. High-resolution flow simulations also allow the designer to model complex flow physics that may reveal unanticipated phenomena before these phenomenon force costly design changes.

Factor ranking and high resolution flow simulations are not new aerospace design tools; however, they commonly are not combined for studying conceptual air vehicle designs due to conceptual designs requiring the assessment of possibly thousands of design trade studies. Typically this volume of design trade studies are managed through rules-of-thumb, low-fidelity flow simulations, and coarse vehicle models.

Rules-of-thumb accommodate the numerous design iterations in the conceptual design phase by allowing many designs to be analyzed in a short amount of time [5]. In this context, rules-of-thumb refer to aerodynamic performance models based upon distillations of data obtained over the years through wind tunnel tests and flight tests. For example, a well-known rule-of-thumb from aerospace engineering is the area rule, which comes in transonic and supersonic versions [6].[2] The transonic area rule states that the cross-sectional area of an air vehicle should vary smoothly from fore to aft in an effort to reduce drag as the speed of sound is approached. The supersonic version is similar in form, but involves projections of the cross-sectional area in an effort to reduce wave drag that arises only at supersonic velocities. Rules-of-thumb, such as the area rule, are often amalgams of empirical knowledge and conceptual insight into the underlying flow physics, but they do not provide the quantitative physics-based information necessary for optimizing the aerodynamic configuration of a particular design in order to achieve new performance capabilities. Additionally, when rules-of-thumb are used to extrapolate beyond their historical bases, they can fail without warning [7].

Low-fidelity computational models can provide a broader range of applicability and more detailed information than rules-of-thumb, as well as more timely simulations than physics-based models. A hypersonic example of a low-fidelity model is the modified Newtonian sine-squared

[2] Transonic flight is the region from approximately 0.8 to 1.0 times the speed of sound. Supersonic flight is the region from one to five times the speed of sound.

model. While this model admits rapid solutions, it is not based upon the differential equations that are accepted to represent a fluid's flow, but upon a somewhat misguided physical model that happens to approximately match the actual flow results observed at high hypersonic speeds [8]. Furthermore, the Newtonian model is only justified for simple shapes [9]. Low-fidelity models are justified only in the benign operating regimes in which the physics is simple enough to admit mathematically convenient simplifications, such as ideal flow models of low speed aerodynamics or high hypersonic speeds around simple shapes.

Although they may provide faster computational solutions, the restricted validity of rules-of-thumb and low-fidelity models commonly result in new vehicle designs that tend to be deviate only slightly from previous designs; consequently, the drawbacks of the old designs become incorporated into the new design. These tools' restricted validity has two related and potentially unfortunate consequences for the design of hypersonic vehicles: (1) extrapolation from previous design configurations is relatively poorly informed in the early design stages and therefore risky, and (2) design choices are biased against innovative configurations and designs which may provide advances towards the objectives of hypersonic flight.

Conceptual design of hypersonic vehicles using computational models has been pursued primarily using coarse vehicle models. An example of a coarse vehicle model used in previous work can be found in Ref. 10. Such models are not representative of an operational vehicle and therefore lack sufficient geometric detail to accurately predict the practical performance of realistic configurations [10-12].

These design studies, while assessing the interaction of structural, aerodynamic, and aerothermal design of a vehicle, neglect the physical fidelity of the vehicle and computational models used in favor of producing results in a timely manner [12]. This neglect is merely a

product of the computational tools available at the time the previous work was completed. New computational tools can combine the rapid parametric design surveys of previous works with more accurate and dependable physics-based simulations. This is the main purpose of the present study.

Typical design studies of hypersonic vehicles rely upon rules-of-thumb, low-fidelity flow simulation tools, and coarse vehicle models. The use of these tools can lead to design decisions being made that may not be able to assess the aerodynamic interactions among the whole range of design variables, thereby limiting the knowledge available to the designer when the design is subject to conflicting constraints. Additionally, the use of low-fidelity tools can lead to unanticipated phenomena occurring later in the design process, possibly after prototype production and testing has already begun. Reducing the shortcomings and pitfalls inherent to the design tools used for hypersonic air vehicle design is an essential step towards overcoming the technical challenges associated with hypersonic flight. Doing so will support the practical goals of designing less expensive and more dependable hypersonic air vehicles.

b) Purpose

The purpose of this research was to determine the feasibility of integrating high-fidelity geometry modeling tools and physically-accurate flow simulations in the conceptual design of air vehicles. The feasibility of these tools was evaluated by performing a global sensitivity analysis of the vehicle's aerodynamics to changes in the vehicles geometry.

2) Methodology

To achieve the technical goals of this research, a framework was developed that was capable of rapidly translating changes in a vehicle's geometry to changes in the vehicle's aerodynamic performance. The framework consisted of four components as shown in Figure 1.

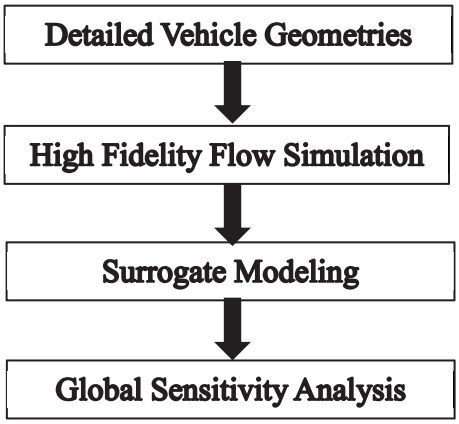

Figure 1. Sensitivity analysis framework overview

The framework was designed to require as little human intervention as possible at all stages including design space generation, volumetric mesh generation, and flow solution convergence monitoring. The framework was designed to avoid any expectation of the user having expertise in the fields of mesh generation or flow simulation. Additionally, the framework was developed to use open source software where feasible to avoid costly licensing issues. The framework was also developed to allow future integration with other analysis tools such as finite element modeling or aerothermal modeling.

a) Detailed Vehicle Geometry Modeling

The creation of a large design space of high-resolution geometry models is crucial to the performance of sensitivity studies of sufficient detail. High resolution geometry models, as

opposed to coarse geometry models, are necessary to capture the detail of a proposed design in order to compute more accurate flow solutions later in the framework.

OpenVSP was used to create the vehicle models and design space [14]. OpenVSP is an open-source parametric geometry modeler designed for the Windows operating system capable of generating high-resolution models capable of export to computational fluid dynamics (CFD) tools. The components and parameters used in OpenVSP reflect the typical component definitions used in the aerospace engineering community, e.g. the fuselage of an aircraft is represented by a "fuselage" component. An example showing the creation of a wing and the available parameters is shown in Figure 2.[3]

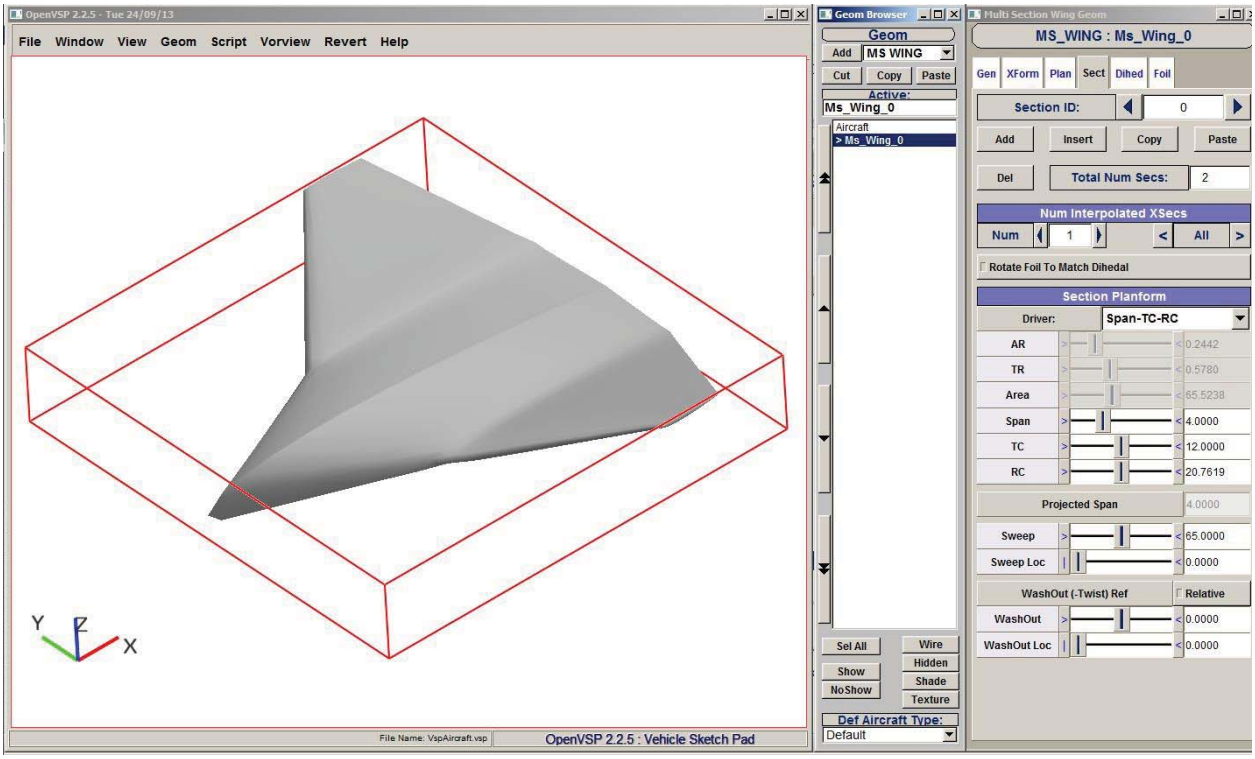

Figure 2. Example multi-section wing in OpenVSP. The right most pane shows the sliders for adjusting the wing's geometric parameters of span, tip chord, and root chord, as well as other parameters used to define the wing's planform and cross-section.

[3] The parameters by which one can define a wing include aspect ratio, taper ratio, and area.

The use of common aerospace nomenclature for components and parameters is in contrast to other computer aided design (CAD) tools, which would require a fuselage to be pieced together from a series of cylinders and cubes. The nomenclature used by OpenVSP is similar to that of the aerospace engineering community and this overlap increases the speed of detailed model generation when compared to CAD tools such as AutoCAD [15]. This speed meets the requirement for rapid turnaround for exploring many design iterations in the conceptual design stage. The parameter based definition of components in OpenVSP also allows the user to create higher resolution models when compared to other CAD tools [15].

The rationale for choosing OpenVSP is also because of OpenVSP's capabilities for output to CFD codes. OpenVSP provides the functionality to compute the internal features and intersections of a model's components in order to create a watertight model suitable for export to a variety of CFD programs.[4] The exported models discard the quadrilateral representation of the model's surface and instead use a triangular representation to facilitate the application of CFD codes to the model. The output of triangular based meshes is merely a result of the majority of CFD tools requiring triangular surfaces for volume mesh generation [16].

The speed at which a single model in OpenVSP can be generated by hand already lends itself to the creation of a large design space of models. The creation of the many models needed to explore a design space was accelerated and automated through the use of two key features of OpenVSP: (1) design files and (2) batch file execution. Plain-text design files in OpenVSP allow the user to specify the component parameters of a baseline model which he/she would like to change. These parameters can then be modified in any text editor. The modified design file can then be loaded into OpenVSP to generate a new geometry model. Batch file execution allows the

[4] Watertight refers to the absence of open curves on the model. Simply put, if the model were filled with water, no leaks would be present.

user to execute OpenVSP commands without starting the graphical user interface (GUI). Bypassing the GUI enables the user to compute and export a mesh suitable for CFD analysis from the command line. Combining design files and batch file execution allows the user to change a baseline model through a modified design file and generate a new model without accessing the GUI of OpenVSP. The combination of these two features greatly accelerates the creation of the geometry models needed for a conceptual design studies where numerous design possibilities must be evaluated. A flowchart showing the process from baseline model to modified model is shown in Figure 3. The automation of design file modifications and model generation was accomplished through a MATLAB script.

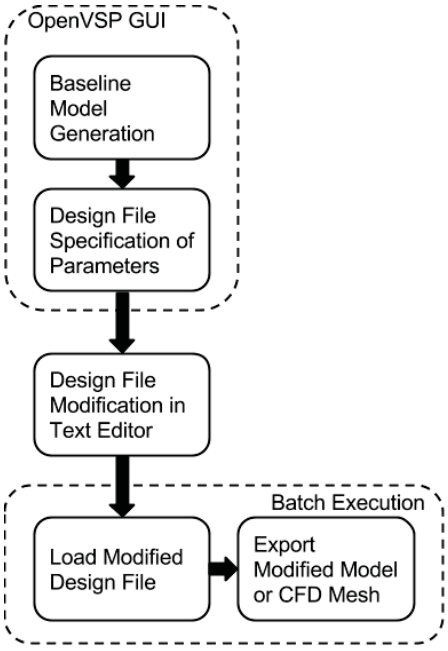

Figure 3. OpenVSP model modification workflow

b) High Fidelity Flow Simulation

To fulfill the objective of producing physically accurate results in the conceptual design stage, the flow around a given air vehicle geometry was simulated more accurately than is commonly the case in current conceptual design tools (e.g., low-fidelity computational models). Cart3D was selected to meet this objective. Cart3D is an Euler flow solver suitable for simulating steady-state inviscid, subsonic-to-hypersonic aerodynamics in the conceptual and preliminary design stages [17]. [5,6,7] Cart3D utilizes advanced volumetric grids and a number of high-resolution CFD techniques to increase the rate of convergence and ensure physically accurate solutions are computed reliably with minimal intervention by the user.

Cart3D's flow solver is not capable of simulating some of the features of hypersonic flow such as real gas effects and chemically reactive flows that are encountered at higher hypersonic speeds. However, based on previous applications of Cart3D it was determined that the modeling of these effects would not be necessary. Previous work completed by AFRL involving the prediction of HiFire and X-51 aerodynamic loads in the hypersonic regime used Cart3D without modifications to account for real gas effects or chemically reactive flows [18-20].[8] Cart 3D was used in the development of the HiFire vehicle to determine its outer mold line from a large database of flow simulations. The X-51 development program used Cart3D to compute the aerodynamic loads throughout the trajectory to facilitate structural sizing. These examples highlight the applicability of Cart3D to the hypersonic regime.

---

[5] Steady-state refers to the time-independence of the flow parameters. An example of steady flow would be an airplane established in cruise.

[6] Inviscid refers to the case where the velocity of the fluid close to the body does not vary from the flow directly above it.

[7] The author would like to acknowledge Mr. Don Garner and Ms. Linda Adlum for their assistance in the installation, setup, and technical support of Cart3D.

[8] HiFire and the X-51 are two hypersonic air vehicles which have undergone flight testing in 2012 and 2013, respectively.

The advanced volumetric grids used by Cart3D utilize automated adaptive refinement and unstructured Cartesian body fitting. Adaptive refinement decreases the volumetric cell volume in regions of high spatial curvature such as the wingtip while unstructured Cartesian body fitting reduces the computational complexity commonly associated with volumetric mesh generation. The use of these two grid methods decreases the computation time and memory requirements of the volumetric grid while still retaining the necessary resolution for physically accurate solutions [21]. The algorithms by which Cart3D handles the intersection of the volumetric grid cells and the solid boundary allow the volume grid generation to be automated and completed in a short period of time [22-23]. The automated generation and adaptive refinement of Cart3D's volumetric meshes met the objective of the framework to require as little human intervention as possible. Additionally, the automated mesh generation used by Cart3D makes it particularly suited for use by vehicle designers that are not expert in mesh generation.

The volumetric mesh in Cart3D can also be adapted to ensure the accuracy of output aerodynamic forces and aerodynamic coefficients through the included adjoint-based mesh adaptation capability. Adjoint-based mesh adaptation in Cart3D is another grid refinement method that creates smaller volumetric cells to improve the accuracy of the output aerodynamic forces [23]. The adjoint-based mesh adaptation built into Cart3D allows the user to specify aerodynamic results of interest, e.g. lift and drag, and minimize the error resulting from coarse cells in the output aerodynamic loads. Volumetric cells that contribute to this error are identified and refined to minimize this error in the integrated quantities. The details of the algorithm that identifies these cells and measures their contribution to the error in aerodynamic force and moment coefficients can be found in Ref. 24. Adjoint-based mesh adaptation allows a user with limited expertise in grid generation to generate a high resolution volumetric grid that ensures an

accurate solution. The limited expertise required helps to fulfill the research objectives by providing a CFD analyses that can be setup and executed in a timely manner. Figure 4 is an example of the adjoint-based mesh adaptation that shows the coarse volumetric mesh for a hypersonic vehicle before and the refined volumetric mesh after the final round of adjoint-based mesh adaptation. The upper left insert in Figure 4 shows the initial coarse volumetric mesh.

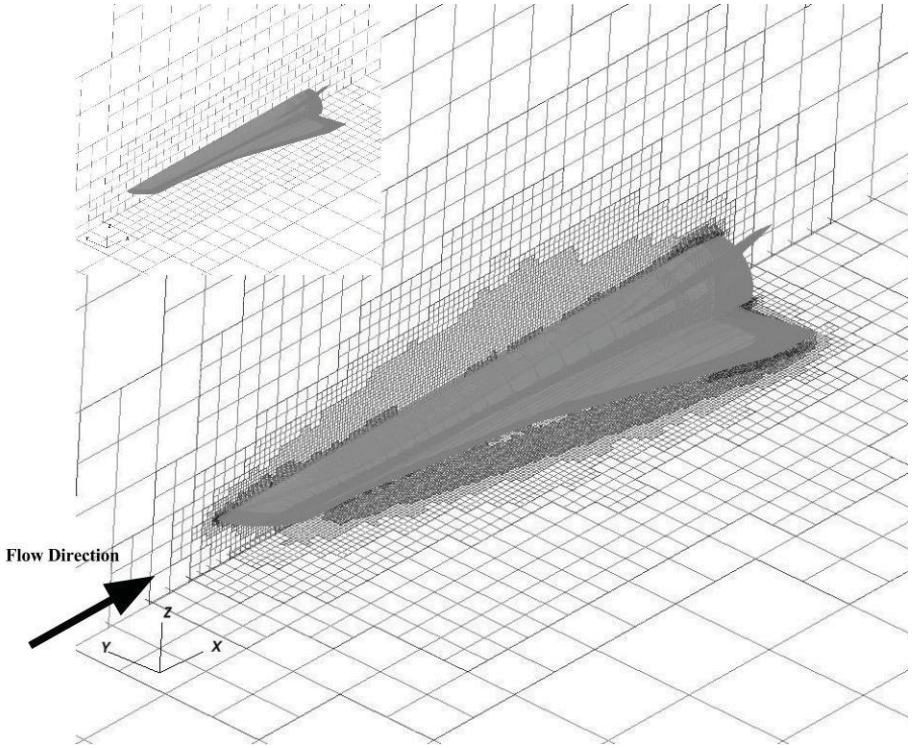

Figure 4- Results of adjoint-based mesh adaptation. The additional mesh resolution in the vicinity of the leading edge of the wing is necessary to resolve a shockwave that forms at hypersonic speeds.

Cart3D also uses a number of high-resolution CFD techniques to capture shockwaves accurately, reduce computation time, and minimize high frequency errors.[9] Cart3D accomplishes these tasks through the use of flux-limiting functions and multigrid methods. A theoretical discussion of flux-limiting functions and multigrid methods can be found in Ref. 25. The two

[9] The errors referred to here are spurious spatial oscillations that often occur in flow solutions with discontinuities such as shockwaves.

aforementioned techniques ensure accurate numerical solutions at high Mach numbers while limiting the computational cost.

A limiting feature of Cart3D is the omission of viscous effects from its solution.[10] Other CFD methods such as a Reynolds-averaged Navier-Stokes solver or a Direct Numerical Simulation of the Navier-Stokes equations would include viscous effects and turbulence. These other flow solution methods could provide more accurate models of certain flow features; however, this increase in physical fidelity would require much greater computational time and resources. The use of these other flow solution methods would also require greater numerical modeling insight from the user. These traits make these high-fidelity methods unsuitable for the conceptual design stage, where a large design space must be assessed. The modular nature of the framework would allow a designer to implement these higher-resolution flow solution schemes should they be desired. In addition, one of the goals of the framework was to allow use of the framework by designers that are not experts in the intricacies of current CFD methods.

c) Post-Processing of Results

Cart3D includes *CLiC*, a force and moment extraction program that resolves the pressure distribution on the air vehicle into body-centered forces. *CLiC* provides the ability to specify moments about points, lines, or along the boundary of a vehicle component such as a rudder. These forces are then written to a text-file that was used in the generation of the surrogate model.

[10] Viscous effects refer to aerodynamic phenomenon such as a boundary layer. A boundary layer is a layer of fluid near the vehicle's body where the velocity varies nonlinearly. The inclusion of a boundary layer leads to more accurate predictions of aerodynamic loads.

d) Surrogate Model Generation

While Cart3D may be able to generate flow solutions more rapidly than previous inviscid flow solvers, the computation time required still prohibits the analysis of every possible design permutation. In order to overcome this computational limit, a surrogate model of the vehicle's aerodynamic response was generated. This surrogate model allowed the interpolation of the vehicle's aerodynamics at design cases that were not directly simulated using Cart3D.

To generate the surrogate model, the DACE toolkit for MATLAB was used [26]. DACE was chosen due it's availability as open source software and the variety of surrogate modeling methods it provides. For this research, a Kriging method was chosen to generate the surrogate model.

Kriging models the correlation between data points as a normal distribution. A full development of the Kriging method can be found in Ref. 27. As a result of this correlation method, Kriging models provide a measure of the uncertainty in the surrogate model across the design space. The designer is then able to determine if more samples of the design space are needed if the level of uncertainty is outside acceptable limits. Additionally, Kriging exhibits better curve fitting than methods such as a cubic spline [27-28]. A simple comparison illustrating this difference is shown in Figure 5.

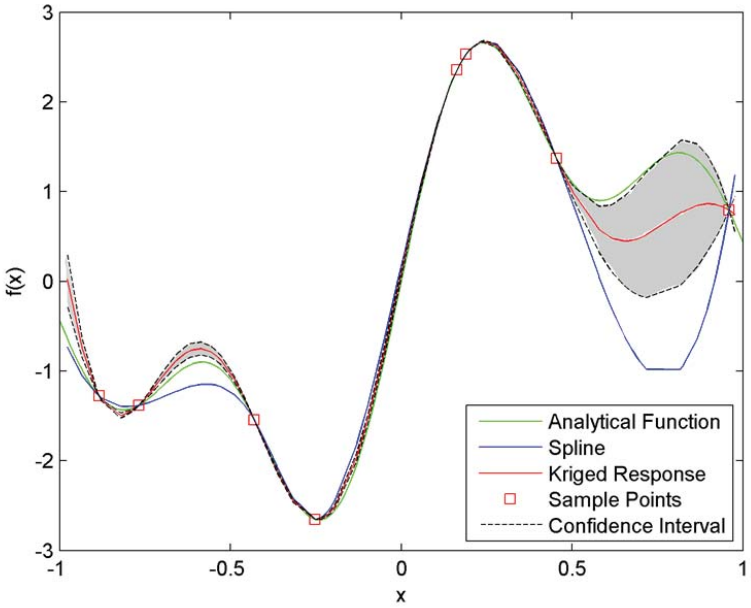

Figure 5. Comparison of interpolation methods.

The analytical function in Figure 5 was:

$$f(x) = \sin(9x) + \sin(5x) + \sin(3x) + \sin(x) \qquad \text{Eqn. (1)}$$

The sample points used for both interpolation methods were generated using MATLAB's pseudorandom number generator to generate eight values of x on the interval $-1 \le x \le 1$. While this example may be simple, it showcases the benefits of a Kriging method when compared to simpler interpolation methods such as cubic spline.

e) Sensitivity Analysis Method

The sensitivity analysis of the vehicle's aerodynamics was performed using an Extended Fourier Amplitude Sensitivity Test (eFAST). A detailed explanation of the algorithm for eFAST can be found in Ref. 29. eFAST is variance based sensitivity analysis that is capable of calculating the first order and total sensitivities of a model. A first order sensitivity is a measure of the variation of model output that can be ascribed to the variation in a single model input. A

total sensitivity is a measure of the variation of model output that can be ascribed to effects that include but are not limited to a specified model input. An example of these effects would be the interaction of two or more model inputs such as the interaction of a wing's leading edge sweep and a wing's airfoil section. For example, six sensitivity indices could be calculated for a model that takes three inputs: three first order (S_1, S_3, S_3) and three total sensitivity indices (S_{T1}, S_{T2}, S_{T3}).

The sensitivity indices take values ranging from zero to one. A model input with a high sensitivity index indicates a factor that is responsible for a large degree of variation in the model output while a model input with a low sensitivity index indicates a factor that is responsible for very little of the variation in the model output. For example, if were interested in a model that predicted the range of an airplane, one would expect the wing geometry to have a high sensitivity index while the choice of interior upholstery would have a low, if not zero, sensitivity index.

An additional feature of sensitivity indices is their ability to predict the interaction of model inputs based on the summation of the first order sensitivity indices. If the summation of first order sensitivities is exactly one, the model is known as an additive model. A non-additive model would be a model where the variance in model output is not solely the summation of the variance in the model inputs.

f) Hypersonic Vehicle Model

The vehicle chosen for the sensitivity analysis was the Generic Hypersonic Vehicle (GHV) provided by AFRL. A three view rendering of the GHV is provided in Figure 6.

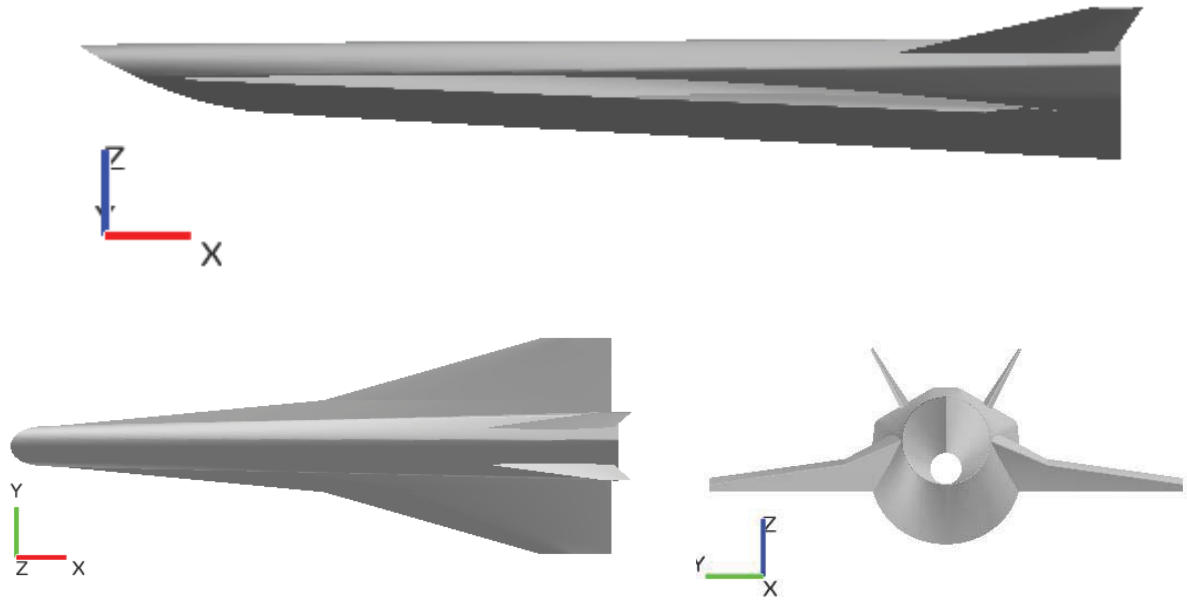

Figure 7. Three view of GHV as provided by AFRL

The GHV similar to many hypersonic vehicles contains an integrated scramjet flow path, a wave-riding fuselage, and deflectable control surfaces. These features differentiate the GHV from previous coarse hypersonic vehicle models where the integration of the propulsion system and control surfaces was neglected [9-10].

The GHV geometry provided by AFRL was manually imported into OpenVSP by fitting OpenVSP components to the point-cloud model. For example, the wing geometry from AFRL was imported into OpenVSP where an OpenVSP multi-section wing component was overlaid. The parameters of the OpenVSP multi-section wing were then manually manipulated until the geometries coincided. The results of this process are shown in Figure 8. For clarity, the vehicle model provided by AFRL will be referred to as AFRL_GHV while the model that was created by the author in OpenVSP will be referred to as USNA_GHV.

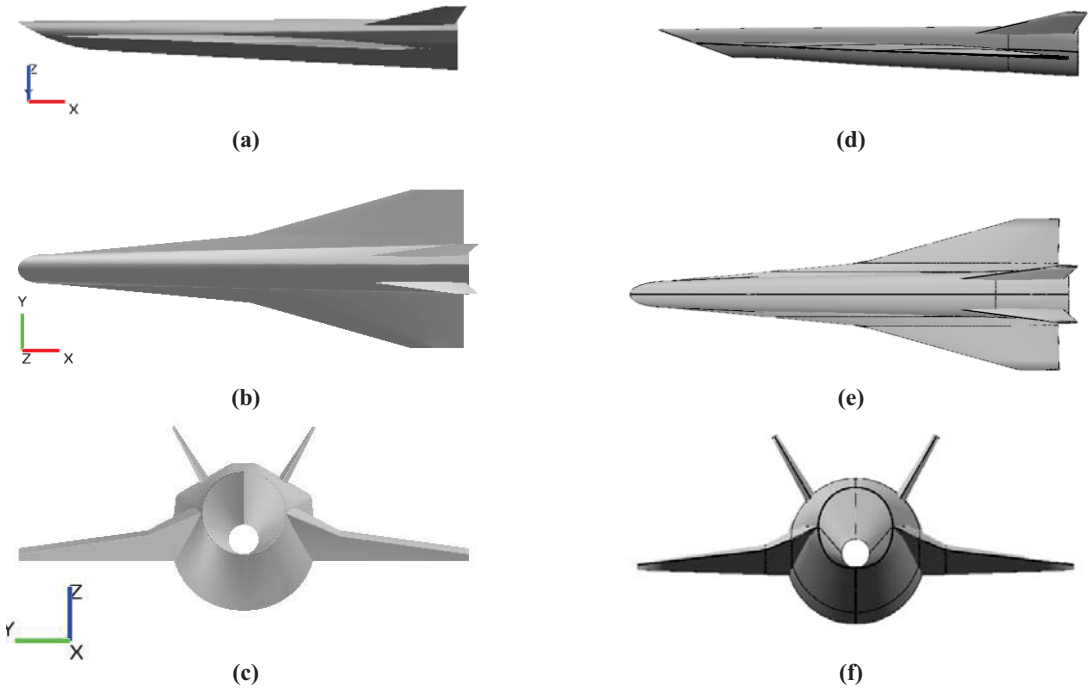

Figure 8. Comparison of the AFRL_GHV model, (a) through (c), and USNA_GHV model manually imported into OpenVSP, (d) through (f).

This manual importing process provided a very good level of agreement between the fins and wings of the OpenVSP GHV model. However, features of the AFRL_GHV's inlet and nozzle were unable to be modeled to the same level of detail as the wings and fins. The assessment of the model fit was based on a qualitative assessment performed when the finished components were overlaid on top of their source components.

OpenVSP's fuselage component is limited to modeling planar cross-sections and does not grant the user the capability to manipulate the Bezier curves that define fuselage cross-sections. As a result of these limitations, OpenVSP was unable to properly model the AFRL_GHV inlet. A detailed view of the AFRL_GHV inlet highlighting the non-planar inlet is shown in Figure and 10. The inlet as modeled in OpenVSP is shown in Figures 11 and 12. The AFRL_GHV empennage, like the inlet, had to be changed from the AFRL_GHV specifications in order to meet the limitations of OpenVSP. Figure 8 (c) highlights the change from the original specification of a semiellipse and pentagon empennage to an entirely elliptical empennage.

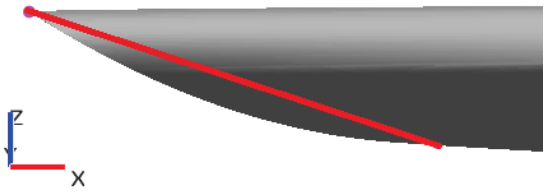

Figure 9. AFRL_GHV Inlet. The red line connects the leading edge and the cusp of the inlet. The cusp is circled in Figure

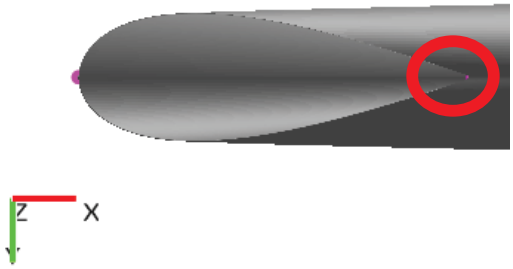

Figure 10. AFRL_GHV Inlet. The red line in Figure connects the pink dot and the cusp, circled in red.

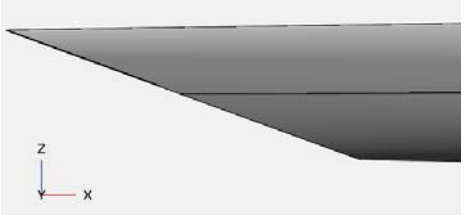

Figure 11. USNA_GHV inlet modeled in OpenVSP showing the planar cross section

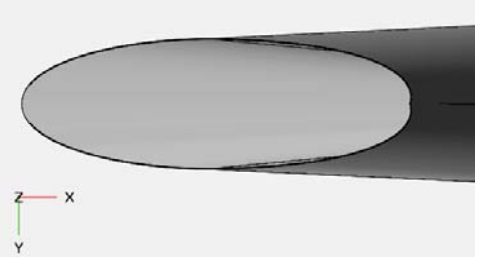

Figure 12. USNA_GHV inlet modeled in OpenVSP showing the limitations of the cross-section manipulation available to the user.

g) Design Space Creation and Sampling

The design space for the sensitivity analysis contained models with parametric variations chosen by a Latin hypercube sampling (LHS) scheme. LHS methods seek to ensure the sample space is sampled uniformly in each design variable with as few samples as possible [27]. The goal is to solve the fewest necessary models to infer a quantitative relationship between the design variables and the aerodynamic performance metrics of interest. Using as few simulations as possible is essential to computationally efficient computations when the design space is large and multiple design parameters are specified, as is the case in the conceptual design stage. An example of a LHS sampling for two design variables, ζ_1 and ζ_2, is shown in Figure .

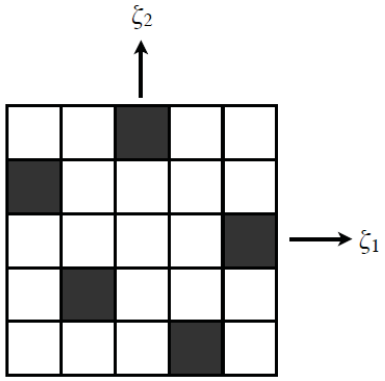

Figure 13. Example of 2D Latin hypercube sampling

h) Combined Sensitivity Study Framework

The tools and methods previously outlined were combined in a framework in order to conduct rapid sensitivity analyses of a hypersonic vehicle's aerodynamic response. MATLAB was used to integrate the separate aspects of the framework. The process of model generation to flow solution is illustrated in Figure 14.

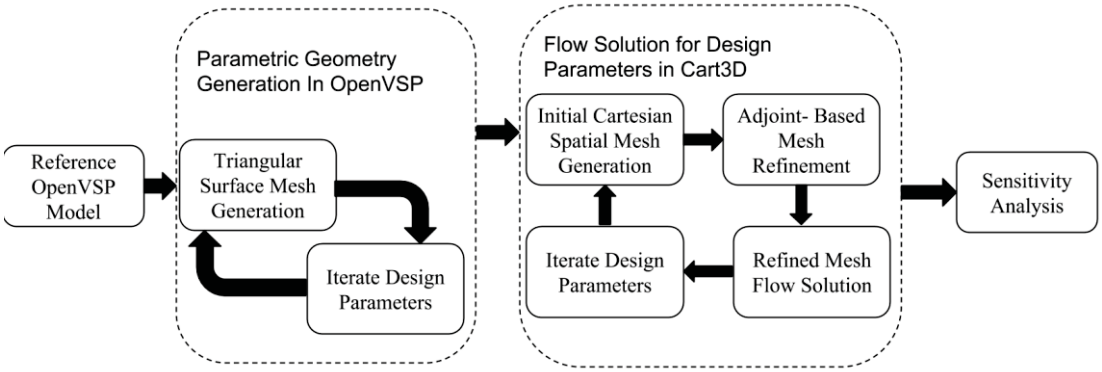

Figure 14. Geometry model generation and flow solution components of sensitivity study framework

The flow solution framework followed these steps (see Figure):

1) Volumetric geometry generation using the surface geometry from OpenVSP
2) Volumetric mesh refinement in areas of high curvature such as the leading and trailing edge.
3) Adjoint-based mesh adaptation. The volumetric mesh will be further refined to reduce the error in the aerodynamic outputs of interest.
4) Export the flow solution to the post-processing software for analyses of computed aerodynamic forces and moments.
5) The above steps will then be repeated for all vehicle designs in the design space.

3) Results and Discussion

a) Validation of SA Framework

The framework outlined in previous sections was validated by performing a simple sensitivity analysis of the ONERA M6 wing's lift curve slope, $C_{L,\alpha}$. This validation was carried out to ensure the framework was capable of computing simple global sensitivities in a simplified flow regime. The ONERA M6 wing was chosen due its wide- spread use as a CFD validation tool. The geometry of the ONERA M6 wing is shown in Figure 9. The design parameters for this validation study were the leading edge sweep angle, Λ_{LE} and the thickness to chord ratio, t/c, also shown in Figure 9. The baseline values for these parameters were 31° and 0.0977, respectively. The design space was bounded to the region:

$$\begin{aligned} 15° \le \Lambda_{LE} \le 45° \\ 0.06 \le t/c \le 0.14 \end{aligned} \qquad \text{Eqn. (2)}$$

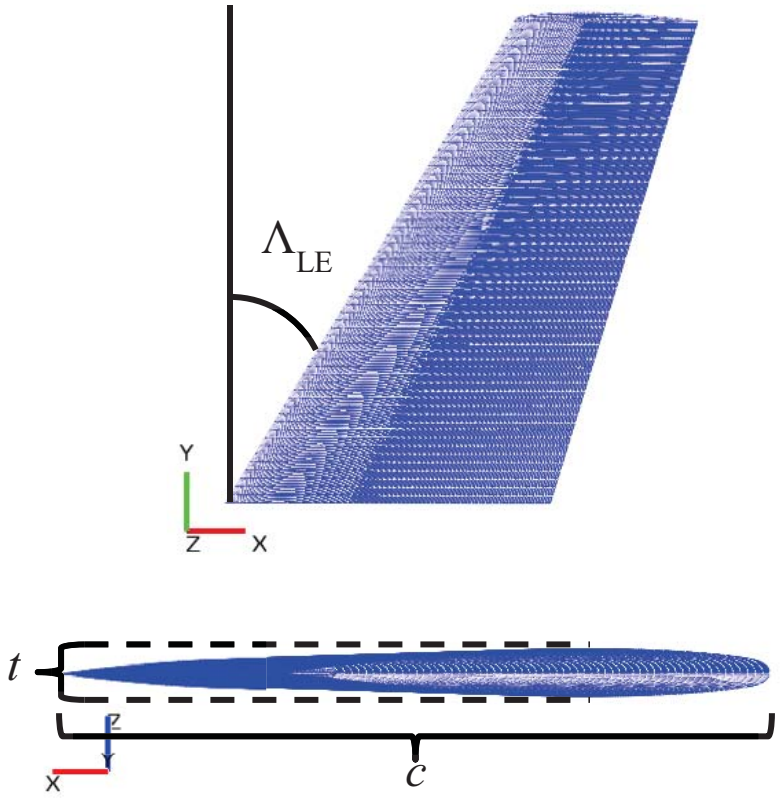

Figure 15. ONERA M6 wing geometry

The design space was sampled at the following 16 points the LHS scheme described in §2.g:

Table 1. ONERA validation study sample points

Sample	t/c	Λ_{LE}
1	0.071033	20.0
2	0.129700	44.0
3	0.060367	38.0
4	0.103033	36.0
5	0.124367	22.0
6	0.119033	42.0
7	0.065700	40.0
8	0.097700	30.0
9	0.081700	34.0
10	0.113700	32.0
11	0.108367	16.0
12	0.135033	26.0
13	0.087033	18.0
14	0.092367	24.0
15	0.076367	28.0
16	0.130000	17.0

The coefficient of lift was computed at $\alpha = 1°, 2°, 3°, 4°, 5°$ and a Mach number of 0.86 using the flow solution method described in §2.b. $C_{L,\alpha}$ was calculated by a least-squares regression of the specified angles of attack and the calculated coefficient of lift. The surrogate model was then calculated using the values of $C_{L,\alpha}$ and the design space samples. The model took the form of:

$$C_{L,\alpha} = C_{L,\alpha}(\Lambda_{LE}, t/c) \qquad \text{Eqn. (3)}$$

The model and its associated uncertainty function were evaluated at 1600 points uniformly sampled in the region given by Eqn. (2). The resulting evaluations and the sample points used to generate the model are presented in Figures 16 and 17.

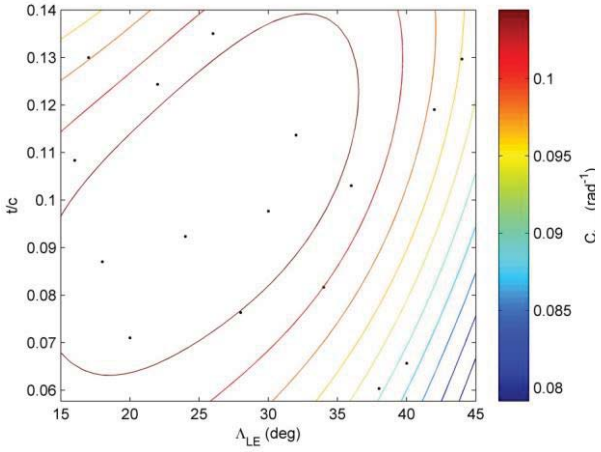

Figure16. Surrogate model of $C_{L,\alpha}$

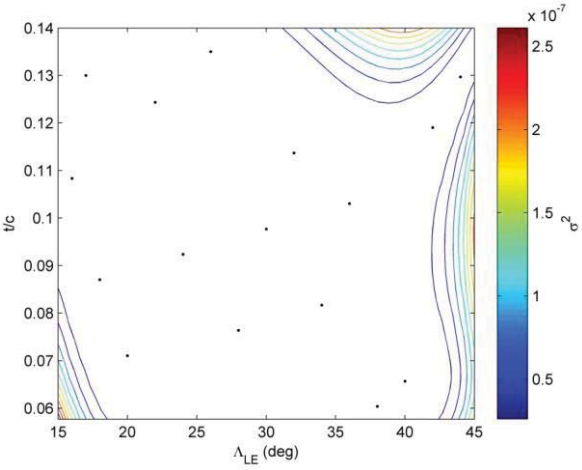

Figure17. Surrogate model uncertainty

As expected, the uncertainty in the surrogate model occurred in regions of the design space where there were not samples taken and the curvature in the model was changing. This behavior is to be expected from the LHS sampling scheme and highlights the well observed fact that LHS schemes sample the design space such that samples are clustered together [30]. The model is also smoothly varying indicating that the calculated model is free from errors in parameter determination. These two results provide a validation for the framework up to the calculation of sensitivity indices.

Using the surrogate model it is possible to qualitatively predict the global sensitivities of the model. As one traverses along the leading edge sweep axis, one encounters many contour lines indicating a rapidly changing $C_{L,\alpha}$. This is in contrast with the trend observed along the t/c axis where the model does not exhibit much variation. From Figure 16, it is also clear that the contours are nearly parallel to the t/c axis at higher leading edge sweep values. This assessment gives a qualitative expectation of how the calculated sensitivities should be ordered.

The calculated sensitivities using the surrogate model are shown in Table 2:

Table 2. Sensitivity indices of the ONERA M6's lift curve slope

	t/c	Λ_{LE}	$\sum_{i=1}^{n} S_i$
Individual Effects (S_1, S_2)	0.1326	0.6562	0.7888
Total Effects (S_{T1}, S_{T2})	0.3317	0.8667	

The calculated first order sensitivities indicate the model is non-additive which is to be expected when compared with historical models that predict a multiplicative relation between the 2D wing characteristics, one of which is t/c, and leading edge sweep such as that provided by Anderson [31]. Additionally, the calculated sensitivity indices confirm the qualitative assessment of the model's sensitivity performed earlier.

The sensitivity analysis framework performed as expected for the simple case of the ONERA M6 wing. This validation study demonstrated the framework provided an automated means to determine the total and individual sensitivities of the ONERA M6's lift curve slope to variations in leading edge sweep and thickness to chord ratio.

b) Two-Parameter Sensitivity Analysis

The USNA_GHV model had a total of over 100 design variables; however, incorporating all of these design variables into a sensitivity analysis would be too computationally expensive for the purpose of testing and initially testing the functionality of the current framework. Additionally, performing a two-parameter sensitivity analysis provided a means to visually assess the Kriging model response surface.

To simplify the design space, only design variables on the wing were chosen for analysis, as these parameters were predicted to have a noticeable impact on the USNA_GHV's L/D ratio. L/D ratio was chosen as it is an important metric in determining the theoretical range of the vehicle. The wing of the USNA_GHV has three distinct wing sections along the span, Figure:

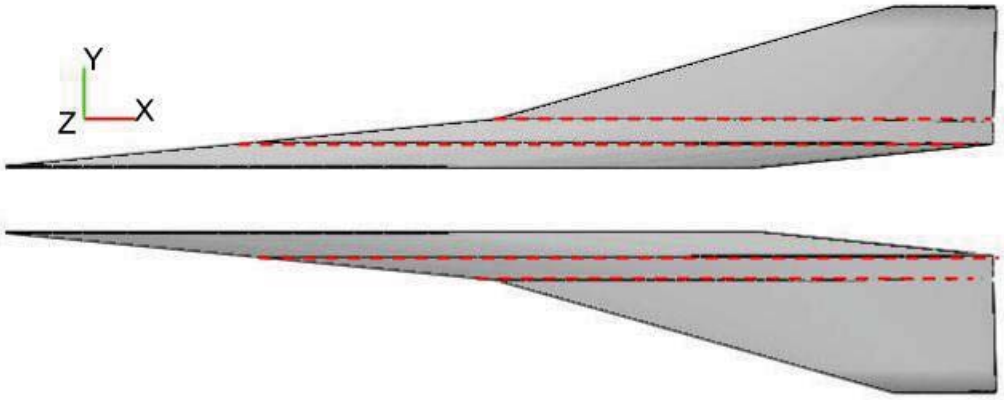

Figure18. USNA_GHV wing. The section breaks are denoted by the red lines

$$\text{Inboard (Section 1): } 0 \le y/b < 0.1587 \qquad \text{Eqn. (4)}$$

$$\text{Middle (Section 2): } 0.1587 \le y/b < 0.3114 \qquad \text{Eqn. (5)}$$

$$\text{Outboard (Section 3): } 0.3114 \le y/b \le 1 \qquad \text{Eqn. (6)}$$

As a proof-of-concept, only the span, b, and dihedral, Γ ,of the outboard section of the wing were allowed to vary. The range of the design variables was chosen such that the extrema were equidistant from the baseline USNA_GHV values

$$\Gamma_{3,0} = -6.5^{\circ}, \Delta\Gamma_3 = \pm 10^{\circ} \Rightarrow \Gamma_3 \in [-16.5^{\circ}, +3.5^{\circ}] \qquad \text{Eqn. (7)}$$

$$b_{3,0} = 17.399 \text{ in}, \Delta b_3 = \pm 3.4798 \text{ in} \Rightarrow b_3 \in [13.9192 \text{ in}, 20.8788 \text{ in}] \qquad \text{Eqn. (8)}$$

The design space was sampled 27 times using LHS as described in §2.g. The resulting design space is shown in Figure.

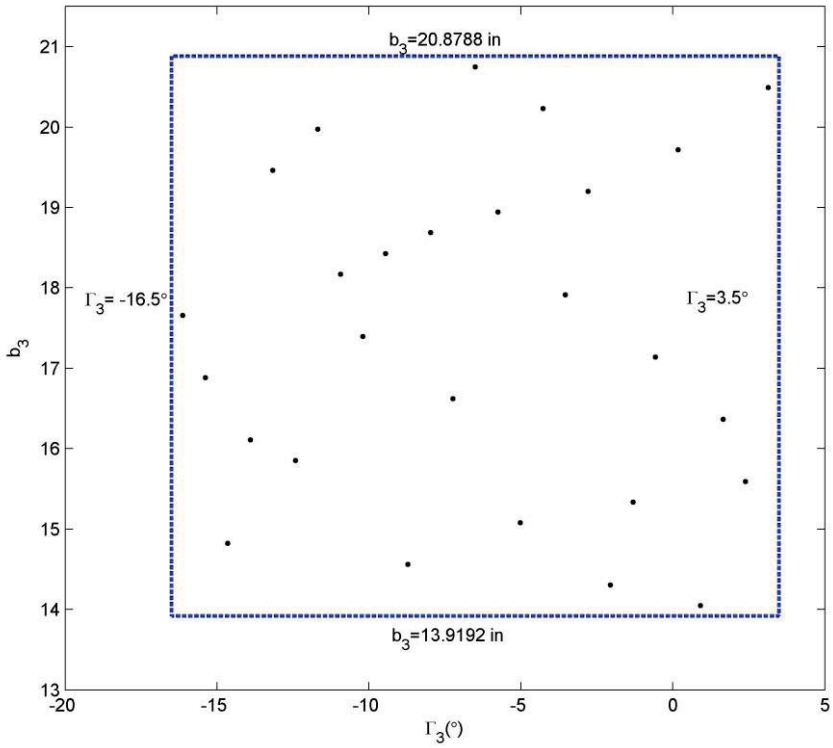

Figure19. Two Parameter Design, 27 Samples

Each surface mesh generated by OpenVSP had approximately 180,000 triangles; this was necessary to ensure the vehicle's surface and the flow domain were discretized with similar resolution after adjoint adaptation of the initial grid (as described below).The GHV was designed to cruise at Mach 6 and at α=0°. This cruise condition was used as the freestream conditions for Cart3D. Studies of the sensitivity of the GHV to variations in α and β were not performed in order to simplify the design space. Cart3D was setup to execute nine levels of adjoint-based mesh refinement for each vehicle model. The lift and drag coefficient of the USNA_GHV were specified as the driving functionals for the adjoint-based mesh refinement. This led to each flow

simulation starting on a mesh of approximately 9000 volumetric cells and ending on a mesh with approximately 3 million cells. A comparison of the starting and final meshes for a representative flow solution is shown in Figures 20 and 21. Although it is not visible in Figures 20 and 21, the scramjet flow path was retained in the vehicle model.

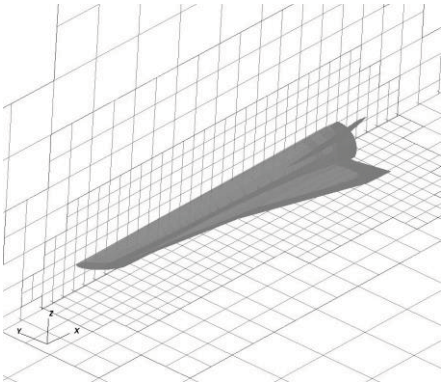

Figure 20. Initial Cart3D volumetric mesh. Shown are only 2-D slices of the 3-D mesh

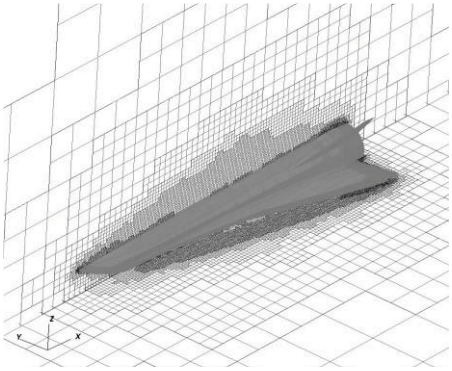

Figure 10. Final Cart3D Volumetric Mesh

The lift and drag coefficients from Cart3D were used to calculate the L/D ratio for each vehicle configuration. A Kriging response surface was fit to the computed L/D ratios using the method described in §2.d. The resulting response surface and the associated model variance are shown in Figure 22a and 22b, respectively.

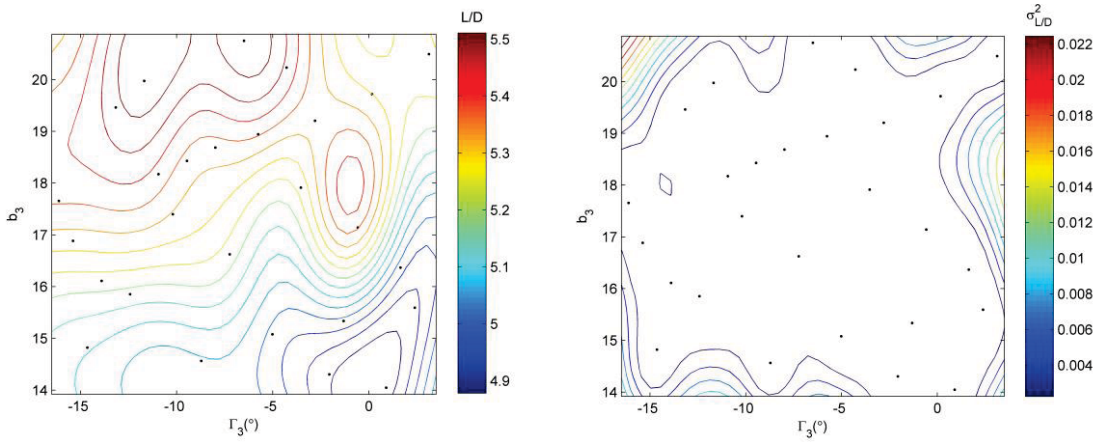

(a) 27- point Kriging response surface **(b) 27- point Kriging response surface variance**

Figure 22. 27-point Kriging response surface

The response surface generated using this initial data set will be referred to as the 27-point response surface. The response surface in Figure 22a has a local maximum in the vicinity of the sample at (-0.6025, 17.13). This maximum seemed abnormal given the curvature of the response surface in the rest of the design space. Three more samples of the design space were chosen at the points (-0.5167, 17.14), (-0.6026, 18.2), and (-0.6026, 18.2) to ascertain whether the sharp rise seen in the response surface was a computational artifact. Additionally, the sample at (-0.6025, 17.13) was removed from the data set. The response surface using the modified design space is shown in Figure 23 and will be referred to as the 29 point response surface. As expected the local maximum in the vicinity of (-0.6025, 17.13) was a computational artifact.

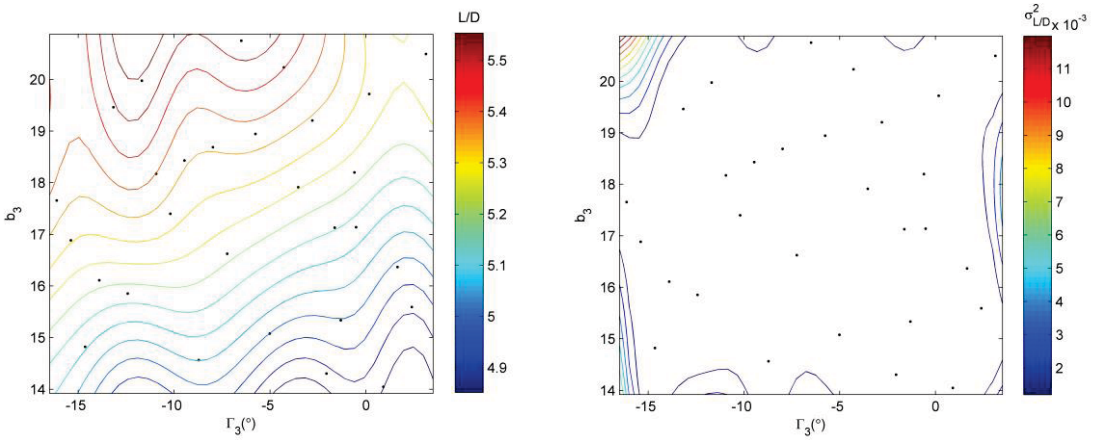

(a) 29- point Kriging response surface **(b) 29- point Kriging response surface variance**

Figure 23. 29-point response surface

In order to evaluate the effects of the computational artifact on the global sensitivity indices, the global sensitivities of the surrogate model were computed using the response surface generated from the 29-point sample and the 27-point sample. Due to the random method at which points are sampled from the surrogate model using the eFAST method, the sensitivity indices were computed 3000 times using 2000 samples of the surrogate model. The resulting sensitivity indices are shown in Figures 24 and 25. The median of these separately computed sensitivity indices is shown in Table 3 in order to provide a metric for quantitative comparison. The percent difference in Table 3 is calculated as

$$\%\text{Diff} = 100 * \frac{|S_{27} - S_{29}|}{S_{29}} \qquad \text{Eqn. (9)}$$

Table 3. Comparison of the median sensitivity indices using the 27 and 29-point response surfaces

	$S_{i,27}$	$S_{i,29}$	% Diff.	$S_{T,27}$	$S_{T,29}$	% Diff.
Γ	0.171	0.212	19.34%	0.257	0.229	12.23%
b	0.737	0.769	4.16%	0.824	0.793	3.91%

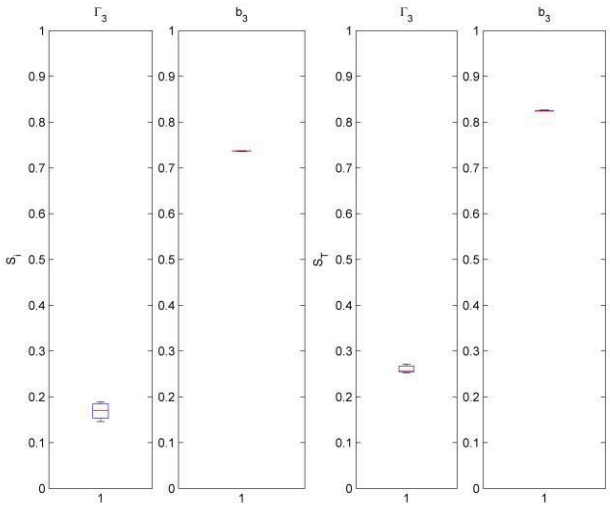

Figure 24. Computed sensitivity indices using the 27-point response surface

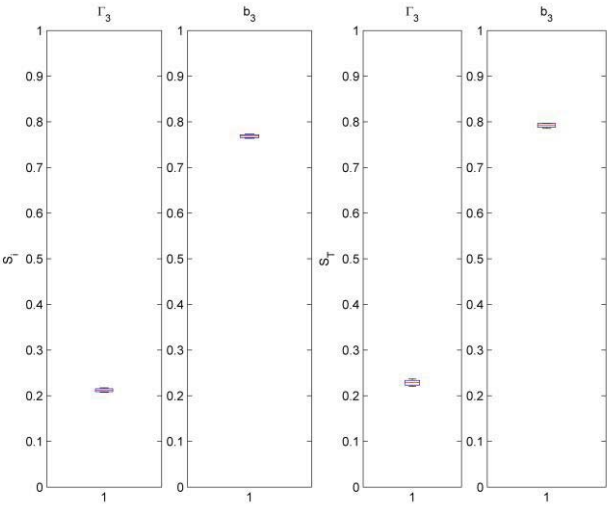

Figure 25. Computed sensitivity indices using the 29-point response surface

While the ranking of the parameters based on their sensitivities did not change based on which data set was used for their calculation, the absolute value of the sensitivities did change. It is conceivable to imagine a scenario where the sensitivity indices were much closer in magnitude and a small change in the magnitude of the sensitivity indices resulting from a computational artifact would lead to a different factor ranking. Such a scenario is more likely to occur in higher-dimensional design spaces where visual identification of computational artifacts is not possible. Two approaches could be taken to alleviate this problem. First, multiple response surface methods could be calculated and compared to determine if any artifacts are skewing the response surface. Second, a response surface methodology that does not interpolate the sample points exactly but instead performs a regression of the design points could be used to mitigate the influence of poorly converged CFD cases on the response surface.

c) Detailed Sensitivity Analysis of the USNA_GHV

Nine parameters where chosen for a detailed sensitivity analysis of the USNA_GHV:

1. Wing mounting angle: θ
2. Dihedral angle of inboard wing section: Γ_1
3. Dihedral angle of middle wing section: Γ_2
4. Dihedral angle of outboard wing section: Γ_3
5. Wing span of inboard wing sections: b_1
6. Wing span of middle wing sections: b_2
7. Fin rotation angle: φ
8. Fin Span: b_f
9. Fin root chord: c_{rf}

The range for each parameter is shown in Table 4 and the parameters are shown on the USNA_GHV in Figures 26-28.

Table 4. Detailed USNA_GHV sensitivity analysis design parameter range

Parameter	Baseline Value	Lower Bound	Upper Bound
θ	0.0°	2.0°	0.4°
Γ_1	-26°	-36°	-16°
Γ_2	-23°	-33°	-13°
Γ_3	-6.5°	-16.5°	3.5°
b_1	4.010 in	3.000 in	4.430 in
b_2	3.860 in	3.000 in	4.414 in
φ	60°	40°	65°
b_f	10.0 in	9.0 in	12.0 in
c_{rf}	39.876 in	30.000 in	41.676 in

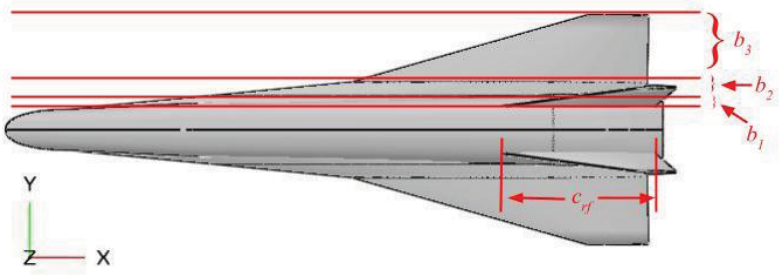

Figure 26. USNA_GHV with design parameters annotated, top view

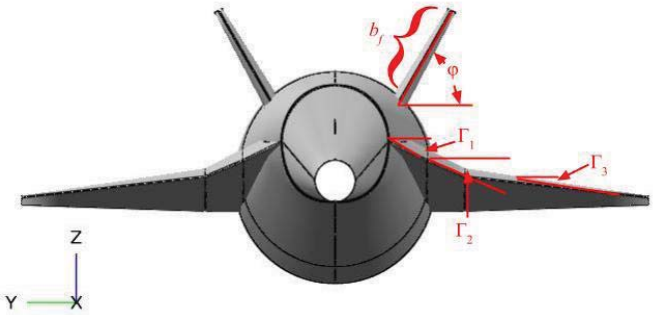

Figure 27. USNA_GHV with design parameters annotated, front view

Figure 28. USNA_GHV with design parameters annotated, left view

90 samples of the design space were taken. This value was determined to be appropriate from the literature that recommends the number of samples be ten times the dimensionality of the design space [27].

Coefficient of lift (C_L), coefficient of drag (C_D), and lift-to-drag ratio (L/D) were calculated using the computational framework. Lift and drag were specified as functionals to drive the solution-based volumetric mesh adaptation. Three of the sample's flow solutions did not converge and were not used in the subsequent sensitivity analysis. Right now there is no indication as to what caused these three cases to not converge. The three cases do not exhibit any unique geometric features that might have caused their surface meshes to be non-watertight. The remaining 87 flow solutions were fed into the previously described sensitivity analysis framework where the sensitivity indices for C_L, C_D, and L/D were calculated 3000 times using 2000 samples of the design space for each sensitivity index calculation. The results are shown in Figures 29-31.

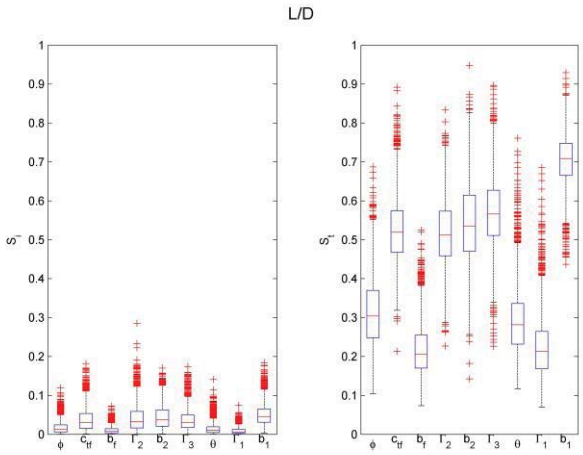

Figure 29. Individual and total sensitivity indices of USNA_GHV's *L/D* ratio

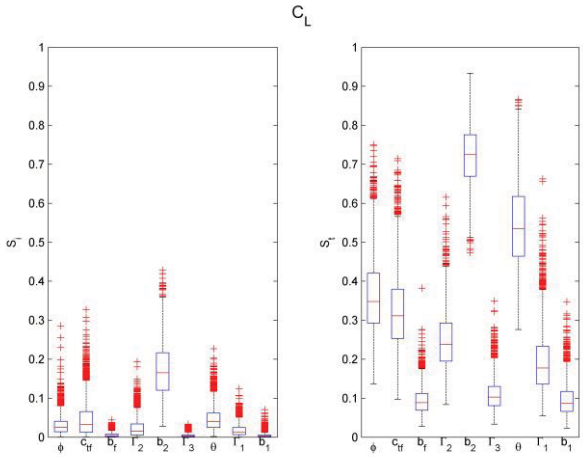

Figure 30. Individual and total sensitivities of USNA_GHV's C_L

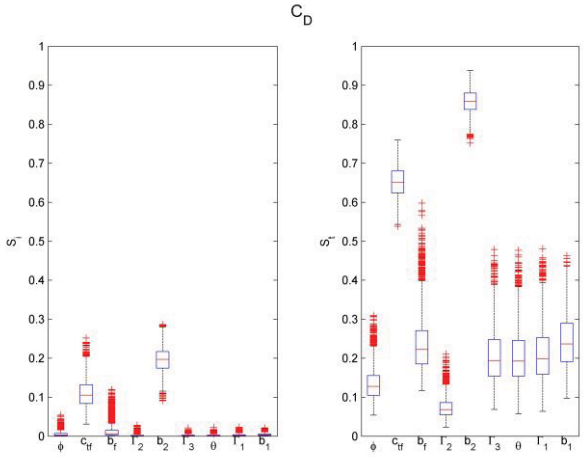

Figure 31. Individual and total sensitivities of USNA_GHV's C_D

The large number of outliers and the skew of the distribution of sensitivity indices suggested possibly improper tuning of the parameters that compose the surrogate model. In particular, DACE creates a Kriging surrogate model using a user-supplied initial value for a correlation parameter, ϑ. DACE then optimizes the correlation parameter to reduce the likelihood estimate of the model, the details of this optimization and the likelihood estimate can be found in Ref. 27. This optimization scheme should arrive at the final value of ϑ regardless of the initial guess. To determine if the surrogate model was the cause of the unexpected distribution of sensitivity indices (Figures 29-31), the sensitivity analysis was performed again using different initial values of ϑ to examine the effect on the sensitivity indices with different initial values and hopefully reign in the variation seen in sensitivity indices and improve the quality of the surrogate model. For economy of space, Figures 32-34 only present the sensitivity indices for C_L. The distribution of sensitivity indices is similar for the other aerodynamic parameters.

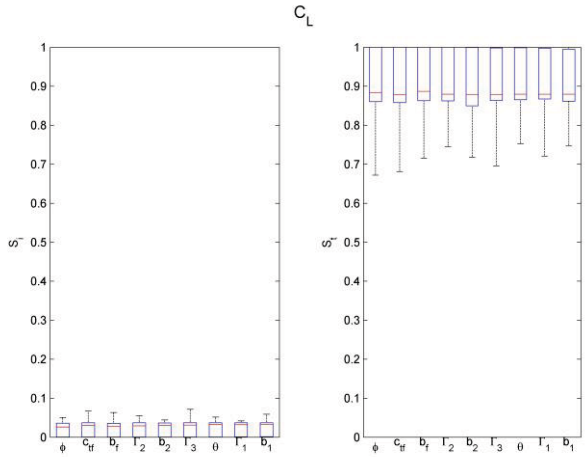

Figure 32. Individual and total sensitivity of USNA_GHV C_L, ϑ = 10

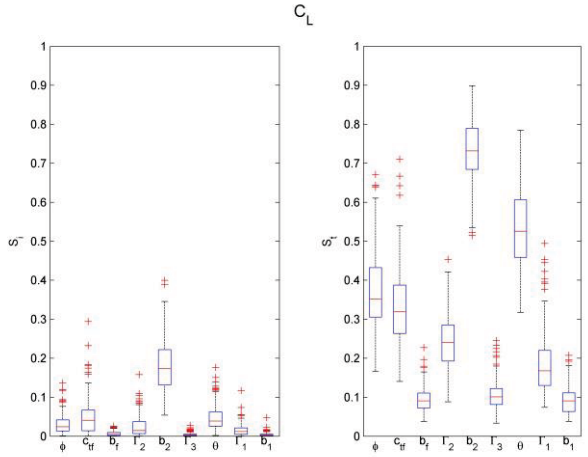

Figure 33. Individual and total sensitivity of USNA_GHV C_L, ϑ = 0.1

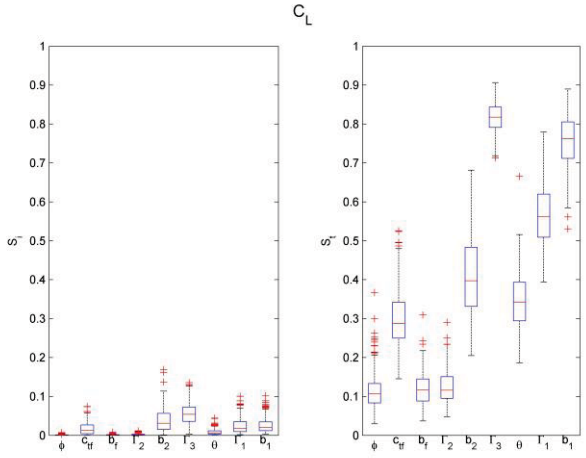

Figure 34. Individual and total sensitivity of USNA_GHV C_L, ϑ = 1

The large variance in the sensitivity indices that results from the user's initial guess of ϑ cast doubt on any simple factor ranking or qualitative assessment of interaction effects of the design factors. From these results, there can be no clear conclusion drawn as to which parameters are most influential on the aerodynamics of a hypersonic vehicle. Additionally, the interaction effects of the design parameters vary wildly with the initial choice of ϑ, thereby preventing any conclusion being drawn as to the interaction of these design factors.

Four factors are currently believed to currently contribute to these inconsistent results:

1. The sampling method used to generate the design space
2. The range of design parameters sampled
3. The choice of Kriging as the surrogate modeling tool
4. The apparently high interaction between the aerodynamic effects of the design parameters caused by non-linear hypersonic flow effects.

The combination of these factors led to the poor performance of the sensitivity analysis framework observed above. The sampling method contributed to the poor performance by spreading the samples across the design space. While this spreading was desirable in trying to economically survey the whole design space, the sparse sampling combined with the large parameter ranges led to a sample set that was found after the fact to not adequately capture the complex interaction among the geometry design variables in this strongly non-linear hypersonic flow application. The too-sparse sample set led to the Kriging surrogate model over-emphasizing the importance of unlikely combinations of the design variables across apparently overly wide sampling intervals. The resulting surrogate model was in effect over-fitting sparse multidimensional data in an application that produced much greater design-variable interactions

than were expected ahead of time. This was finally recognized through the sensitivity indices being unduly influenced by the initial choice of the smoothing parameter.

Future work will focus on completing a detailed build-up of parametric variations to assess the appropriate sample size and parameter range necessary for a detailed sensitivity analysis. The method used herein contains too much uncertainty due to the large parameter ranges and sparse sample size. However, if physically-accurate flow solutions are to be integrated into the conceptual design process, large parameter ranges and sparse sampling schemes must be retained in order to minimize the computational burden from physically-accurate flow simulations. It would be naïve to blindly increase the number of samples and decrease the parameter ranges as this would require excessive computational resources and limit the potential for truly innovative vehicle designs to emerge. Rather, future work should seek to minimize and cope with the uncertainty introduced by the requirements of sparse sampling and large design parameters by incorporating and evaluating regression methods into future iterations of this framework.

4) Conclusions

A highly automated computational framework for the conceptual design of hypersonic air vehicles was developed and demonstrated by performing a detailed sensitivity analysis of a hypersonic air vehicle. The framework incorporated high-fidelity geometry modeling tools and physically-accurate flow simulations. However, the high-fidelity geometry modeling tools were unable to model complex geometric features that are present on the AFRL_GHV and will be present on future vehicles. While the high-fidelity geometry modeling tools provide an advantage over legacy methods in modeling complex vehicle geometries, work should be

undertaken to ensure they are capable of modeling the most general classes of vehicles. Additionally, future work should focus on creating tools that can translate point-cloud type vehicle models into parametric vehicle models in order to increase the interoperability between computational codes. The creation of these tools would also serve to reduce the error that occurs when point-cloud models are translated by hand into parametric models as was the case with importing the AFRL_GHV into OpenVSP.

The framework performed exceedingly well in the simple case of determining the sensitivity of the USNA_GHV's *L/D* ratio in the case of only two geometric parameters varying. The Kriging model did predict a local maximum that was later determined to be a computational artifact. This local maximum was an anomaly and not indicative of a failure of the framework. Future iterations of the framework should include some means to automatically identify such anomalies and modify the surrogate model accordingly.

Despite the framework's performance with two geometric parameters, in the more rigorous case of nine geometric parameters, the framework failed to produce consistent results. The combination of a sparse sampling scheme, large parameter ranges, and the use of simple Kriging for response surface analysis led to an inconclusive detailed sensitivity analysis of the USNA_GHV. The strong non-linearities exhibited by inviscid hypersonic flow led to the creation of response surfaces that do not accurately capture the underlying physical phenomenon and the interaction effects among design variables. Instead, the models created using simple Kriging exhibit a large degree of variation that is captured by the inconsistent nature of the results from the sensitivity analysis. Future work will seek to gain a deeper understanding of appropriate parameter ranges and sampling density. Additionally, other surrogate modeling

methods such as Regression-Kriging will be investigated in order to alleviate the uncertainty but retain the computational efficiency associated with sparsely sampled design spaces.

Glossary

Aerodynamic Loads: the forces and moments exerted on a body resulting from differential pressures and shear forces on the body. Example aerodynamic loads include lift and drag.

Aerothermal Effects: the heating of a fluid medium resulting from compression or expansion of the medium. These effects become a significant consideration at hypersonic velocities.

Computational Fluid Dynamics (CFD): the use of computers to predict the flow parameters and forces an air vehicle would experience in flight.

Computational Framework: an assembly of various software programs into a unified configuration that enables the output of one piece of software to be used as an input into the next piece of software in the framework with little human interaction.

Conceptual Design Phase: the first design phase of an air vehicle. The goals of this phase are typically determining the geometry, performance, and weight of air vehicle. Of primary concern is determining if the vehicle is capable of meeting the specified performance requirements. Examples of performance requirements include range, maximum velocity, and landing distance.

Control Surfaces: surfaces on the air vehicle which are capable of altering the direction of flight. Examples include ailerons, rudders, and elevators.

Design Space: the collection of numerous air vehicle designs in which each design varies slightly from the other designs.

Empennage: the aft section of an aircraft. The empennage typically houses the horizontal and vertical tail.

Hypersonic: the flow regime that exists above Mach 5. Characteristics of hypersonic flows include aerodynamic heating, chemically reactive flows, and thin shock layers.

Leading and Trailing Edge: the forward and aft edges of a wing.

Mach Number: the ratio of a velocity to the speed of sound in the medium. For example, a vehicle traveling at Mach 5 is traveling at five times the speed of sound.

Planform: the projected area of a wing or aircraft on a surface horizontal to the wing or aircraft.

Preliminary Design Phase: the second design phase of an air vehicle. This phase is concerned with more detailed analysis of the air vehicle's performance. Additionally detailed analysis of the necessary systems, e.g. internal structure, will be completed.

Response Surfaces: a mathematical approach which allows the correlation of input variables to output variables. In the case of two input variables and a single output variable, the response surface would take the form of a three dimensional surface similar to those in undergraduate courses in multivariable calculus.

Sensitivity Analysis/Studies: the quantification of the degree to which a change in an input variable impacts a given output variable. Sensitivity analysis is concerned with answering questions such as how much does the lift (output) of an air vehicle change as the wingspan (input) is changed.

Subsonic: the flow regime that exists below Mach 1.

Supersonic: the flow regime that exists above Mach 1 and below Mach 5. Characteristics of supersonic flows include the presence of shock layers and the presence of drag caused by the generation of shockwaves.

Surface Mesh: a computer representation of the air vehicle's exterior used in CFD to define the boundary of the air vehicle and the air flow.

Volumetric Grid: the collection of polyhedra surrounding a vehicle and filling the space during CFD. These typically take the form of cubes.

References

[1] P. Butterworth-Hayes, "U.K. advances air-breathing rocket technology," *Aerospace America*, September 2013, pp 4-6.

[2] A. F. Woolf, "Conventional Prompt Global Strike and Long-Range Ballistic Missiles: Background and Issues," Congressional Research Service, April 26, 2013.

[3] Schmisseur, J., 'Hypersonics into the 21st century: A perspective on AFOSR-sponsored research in aerothermodynamics', *Progress in Aerospace Sciences*, vol. 72, Jan. 2015, pp. 3–16.

[4] J. Slotnick, A. Khodadoust, J. Alonso, D. Darmofal, W. Gropp, E. Lurie, and D. Mavriplis, "CFD Vision 2030 Study: A Path to Revolutionary Computational Aerosciences," NASA/CR-2014-218178, 2014.

[5] M. J. Grant and R. D. Braun, "Analytic Hypersonic Aerodynamics for Conceptual Design of Entry Vehicles", in *48th AIAA Aerospace Sciences Meeting*, ed: American Institute of Aeronautics and Astronautics, 2010. Accessed at: http://www.ssdl.gatech.edu/papers/conferencePapers/AIAA-2010-1212.pdf

[6] J.D. Anderson, "Aerodynamics of the Airplane: The Drag Polar," *Aircraft Performance and Design*, 1st ed., McGraw-Hill, New York, 1999, pp.116-119.

[7] J. D. Anderson, "A Philosophy of Conceptual Airplane Design," *Introduction to Flight*, 7th ed., McGraw-Hill, New York, 2012, pp.562-565.

[8] J. D. Anderson, "Newtonian Law for Hypersonic Flow," *Introduction to Flight*, 7th ed., McGraw-Hill, New York, 2012, pp.844-850.

[9] J. J. Bertin and R. M. Cummings, "Newtonian Flow Model," *Aerodynamics for Engineers*, 6th ed., Pearson Education, Saddle River, 2013.

[10] R. McDonald and D. N. Mavris, "Formulation, Realization, and Demonstration of a Process to Generate Aerodynamic Metamodels for Hypersonic Cruise Vehicle Design," in *2000 World Aviation Conference*, ed: American Institute of Aeronautics and Astronautics, San Diego, 2000.

[11] P.W.G. De Baets and D.N. Mavris, "Methodology for the Parametric Structural Conceptual Design of Hypersonic Vehicles," in *2000 World Aviation Conference*, ed: American Institute of Aeronautics and Astronautics, San Diego, 2000.

[12] M. Graham and D. N. Mavris, "Implementation of Parametric Analysis to the Aerodynamic Design of a Hypersonic Strike Fighter," in *2000 World Aviation Conference*, ed: American Institute of Aeronautics and Astronautics, San Diego, 2000.

[13] Ender, T., and McClure, E., 'Development of an Integrated Parametric Environment for Conceptual High Speed Missile Sizing', *AIAA's Aircraft Technology, Integration, and Operations (ATIO) 2002 Technical Forum*, Jan. 2002.

[14] OpenVSP. http://openvsp.org/

[15] W. J. Fredericks, K. R. Antcliff, G. Costa, N. Deshpande, M. D. Moore, E. A. San Miguel, *et. al*., "Aircraft Conceptual Design Using Vehicle Sketch Pad," in *48th AIAA Aerospace Sciences Meeting Including the New Horizons Forum and Aerospace Exposition*, ed: American Institute of Aeronautics and Astronautics, 2010.

[16] S. J. Owen, "A Survey of Unstructured Mesh Generation Technology," in *IMR*, 1998, pp. 239-267. Accessed at http://ima.udg.edu/~sellares/ComGeo/OwenSurv.pdf

[17] Cart3D. http://people.nas.nasa.gov/~aftosmis/cart3d/

[18] K. G. Bowcutt, D. Dolvin, A. Paull, and M. Smart, "HiFire: An International Collaboration to Advance the Science and Technology of Hypersonic Flight," *28th Congress of the International Council of the Aeronautical Sciences*. Brisbane, 2012.

[19] R. Kimmel, D. Adamczak, R. Gosse, K. Berger, and S. Rufer, "Ground Test and Computation of the Boundary Layer Transition on the Hypersonic International Flight Research and Experimentation (HiFire)-5 Vehicle," AFRL-RB-WP-TR-2011-3025.

[20] R. Mutzman, and S. Murphy, "X-51 Development: A Chief Engineer's Perspective," *17th AIAA International Space Planes and Hypersonic Systems and Technologies Conference*, San Francisco, 2011.

[21] M. J. Berger, M. J. Aftosmis, J. Melton - "Accuracy, Adaptive Methods and Complex Geometry" Proc. 1st AFOSR Conference on Dynamic Motion in CFD. Rutgers, NJ , 1996

[22] M. J. Aftosmis, M. J. Berger, and G. Adomavicius, "A Parallel Cartesian Approach for External Aerodynamics of Vehicles with Complex Geometry," *Proceedings of the Thermal and Fluids Analysis Workshop 1999*. NASA Marshall Spaceflight Center, Huntsville, AL, Sep. 1999

[23] M. Nemec, M. J. Aftosmis, and M. Wintzer, "Adjoint-Based Adaptive Mesh Refinement for Complex Geometries," in *46th AIAA Aerospace Sciences Meeting*, ed: American Institute of Aeronautics and Astronautics, Reno, 2008.

[24] M. Nemec and M.J. Aftosmis, "Adjoint Error Estimation and Adaptive Refinement for Embedded-Boundary Cartesian Meshes," in *18th AIAA Computational Fluid Dynamics Conference*, ed: American Institute of Aeronautics and Astronautics, Miami, 2007.

[25] J. D. Anderson, "Some Advanced Topics in Modern CFD: A Discussion," *Computational Fluid Dynamics: The Basics with Applications*, 1st ed., McGraw-Hill, New York, 1995, pp 479-514.

[26] DACE Toolbox. http://www.imm.dtu.dk/~hbni/dace/

[27] A. Forrester, A. Sóbester, and A. Keane, "Kriging," *Engineering Design via Surrogate Modeling*: *A Practice Guide,* 1st ed., John Wiley & Sons Ltd., 2008, pp. 49-63.

[28] Simpson, T. W., Mauery, T. M., Korte, J. J., and Mistree, F., 'Kriging Models for Global Approximation in Simulation-Based Multidisciplinary Design Optimization', *AIAA Journal*, vol. 39, Jan. 2001, pp. 2233–2241.

[29] A. Saltelli, S. Tarantola, and K. P.-S. Chan, "A Quantitative Model-Independent Method for Global Sensitivity Analysis of Model Ouput," in *Technometrics*, Vol. 41, No. 1, February 1999, pp. 39-56.

[30] Romero, V. J., Burkardt, J. V., Gunzburger, M. D., and Peterson, J. S., 'Comparison of pure and "Latinized" centroidal Voronoi tessellation against various other statistical sampling methods', *Reliability Engineering & System Safety*, vol. 91, Jan. 2006, pp. 1266–1280.

[31] J. D. Anderson, "Subsonic Compressible Flow over Airfoils: Linear Theory," *Fundamentals of Aerodynamics*, 5th ed., McGraw-Hill, New York, 2011, pp 741-743.